

Cage Effect, Local Anisotropies, and Dynamic Heterogeneities at the Glass Transition: A Computer Study of Hard Spheres

B. Doliwa and A. Heuer*

Max-Planck Institut für Polymerforschung, Postfach 3148, D-55021 Mainz, Germany

(Received 5 January 1998)

Computer simulations of a hard sphere system close to the glass transition are presented. From three-time correlations, we obtain information about the single-particle dynamics on all relevant time scales, including the presence of dynamic heterogeneities. A detailed picture of the cage effect in the β regime is obtained, yielding information about shape, size, and relaxation properties of the effective cage. Pronounced anisotropic dynamics is mainly observed in the β regime. [S0031-9007(98)06118-3]

PACS numbers: 64.70.Pf, 61.20.Ja, 61.20.Lc, 61.43.Fs

The dynamics of glass forming systems close to the glass transition is very complicated due to its collective nature and results in different relaxation mechanisms [1,2]. During the last few years, many experiments have been performed close to the critical temperature T_c , where the fast β relaxation as well as the α relaxation can be observed. The qualitative picture is as follows: For short times (β regime) a particle is surrounded by an effective cage which keeps the particle close to its original position. Only after a sufficiently long time (α regime) the particle succeeds in leaving the cage.

A formal description of both scenarios can be formulated in the framework of the mode-coupling theory for translational as well as rotational degrees of freedom; see, e.g., [3–6]. Specific predictions are made for the properties of the intermediate scattering function, correlating the density at *two* times. However, due to the complexity of the projection and factorization schemes, additional statements are difficult to obtain. Here we specifically refer to properties of the cage effect as probed by a tagged particle. What is the shape of a typical cage? Up to which time scale can the concept of a cage be used? Is it possible to formulate a simple physical picture of the cage effect? Furthermore, one may ask whether or not the complex relaxation pattern can be interpreted as a superposition of different relaxation rates.

Computer simulations are suitable to obtain specific microscopic information. As has been shown in recent work, from analysis of *three*-time correlations qualitatively new information can be gained, yielding additional insight into the underlying nature of complex dynamic processes [10]. Such correlation functions are also accessible from experiments [7–9]. Among other things, it is possible to determine the *relaxation type* [10]. It distinguishes whether nonexponential relaxation is due to a superposition of exponential processes with different relaxation rates (heterogeneous scenario)—a simple example is an ensemble of diffusing particles with different diffusion constants—or due to intrinsic nonexponentiality (homogeneous scenario). As extensively discussed in [10], the homogeneous scenario can be traced back to correlated back-and-forth

dynamics as expected for the dynamics in a cage. Experimentally, the rotational dynamics in the α regime turns out to be heterogeneous [7–9,11–15].

The goal of this Letter is to obtain a detailed microscopic understanding of the different time regimes at the glass transition. We mainly concentrate on the nature of the cage effect as expressed by the questions raised above. The information is mainly extracted from correlating the position of a tagged particle at three subsequent times $\vec{r}(0)$, $\vec{r}(t)$, and $\vec{r}(2t)$ for different values of t . The simulation is performed for a hard sphere system close to the glass transition density ($\rho = 0.58$) with $N = 1000$ particles. Because of its simplicity, it is an attractive system for computer simulations (see, e.g., [16–19]) and may yield generic features of the glass transition. To some approximation an experimental realization of this system are colloidal suspensions [20]. Because of the polydispersity of $\sigma = 10\%$, crystallization is effectively avoided in the present simulations [21,22]. A Monte Carlo algorithm with a maximum step size of 0.03 (lengths are always given in units of the average radius) is employed, corresponding to an acceptance rate of 50%; see Ref. [18] for more details. We simulated 10^8 Monte Carlo steps (MCS), i.e., $N \times 10^8$ moves. In reality, this corresponds to the time scale of seconds. Data were taken after a sufficiently long equilibration period.

For correlating the dynamics of two subsequent time intervals, we introduce the conditional probability functions $p_{3,\parallel}(\hat{r}_{12}\hat{r}_{01}|r_{01};t)$, and $p_{3,\perp}(\hat{r}_{12}\hat{u}_{01}|r_{01};t)$ with $\vec{r}_{mn} \equiv \vec{r}(nt) - \vec{r}(mt)$, $r_{mn} \equiv |\vec{r}_{mn}|$. Here \vec{u}_{01} is an arbitrary vector orthogonal to \vec{r}_{01} . The hat denotes a unit vector. For later purposes, we abbreviate $x_{12} \equiv \hat{r}_{12}\hat{r}_{01}$ and $y_{12} \equiv \hat{r}_{12}\hat{u}_{01}$. $p_{3,\parallel}(x_{12}|r_{01};t)$ denotes the probability that a particle moves by x_{12} in the second time interval, projected along the direction of the motion in the first time interval, *under the condition* that it moved a distance of r_{01} in the first time interval. In analogy, $p_{3,\perp}(y_{12}|r_{01};t)$ contains information about the motion perpendicular to the motion in the preceding time interval. Only in the case of dynamical processes without memory, i.e., Markovian dynamics, the dynamics in both time intervals would be totally uncorrelated.

In analogy to the discussion in [10], the relaxation type, as introduced above, can be formally defined on the basis of $p_{3,\parallel}(x_{12}|r_{01};t)$ and $p_{3,\perp}(y_{12}|r_{01};t)$ [23]. Note that only for purely exponential relaxation \vec{x}_{01} and \vec{r}_{12} are uncorrelated. In the purely heterogeneous scenario, one has $p_{3,\parallel}(x_{12}|r_{01};t) = p_{3,\parallel}(-x_{12}|r_{01};t)$ so that back-and-forth jumps have the same probability (no *direction* dependence). In contrast, the purely homogeneous scenario is characterized by the lack of any *distance* dependence, hence, excluding the presence of different mobilities. Formally, this implies that $p_{3,\parallel}$ and $p_{3,\perp}$ do not depend on r_{01} . In analogy to Ref. [10], we define $F_2(2t) \equiv \langle \cos \vec{q} \cdot \vec{r}_{02} \rangle$ (the conventional incoherent intermediate scattering function), and $F_3(t,t) \equiv \langle \cos \vec{q} \cdot \vec{r}_{12} \cos \vec{q} \cdot \vec{r}_{01} \rangle$. After a straightforward calculation (see Ref. [10]), one obtains $F_2(t)^2 = F_3(t,t)$ for the purely homogeneous case and $F_3(t,t) = F_2(2t)$ for the purely heterogeneous case.

In Fig. 1, $F_2(t)^2$, $F_3(t,t)$, and $F_2(2t)$, as well as the average mean-square displacement $\sqrt{\langle \Delta r^2(t) \rangle}$, are displayed. The value of $q = 3.1$ is close to the maximum of the structure factor. For the mean-square displacement, one clearly observes three time regimes. The short-time dynamics ($t \ll 100$) is diffusive; i.e., $\langle \Delta r^2 \rangle \propto t$. On intermediate time scales, corresponding to the β regime ($t < 10^5$), subdiffusive dynamics is observed. In the α regime at long times, the dynamics is again diffusive. Because of the close agreement of $F_2(t)^2$ and $F_3(t,t)$, the β regime is mainly homogeneous as expected if the dynamics is strongly influenced by the presence of a cage. In contrast, the α regime is mainly heterogeneous. This shows that the nonexponentiality in the α regime is mainly due to a superposition of diffusion processes with

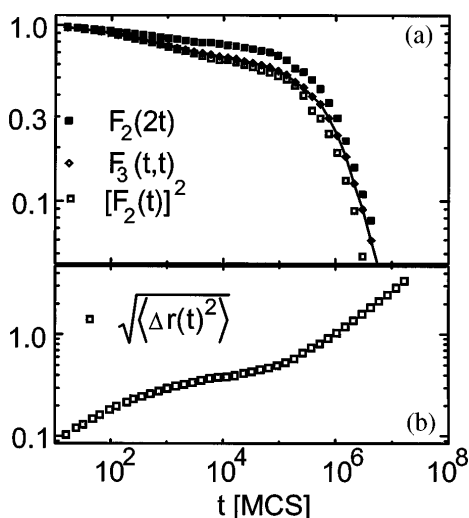


FIG. 1. (a) The two-time and three-time correlation functions $F_2(2t)$ and $F_3(t,t)$ as well as $[F_2(t)]^2$ for q close to the maximum of the structure factor. From the relative positions of the three functions, one can directly deduce that the relaxation type is mainly homogeneous in the β regime and mainly heterogeneous in the α regime. (b) The square root of the mean square displacement.

different diffusion constants, rendering the concept of a rate distribution useful.

Although this analysis is convenient to obtain a first qualitative picture (and experimentally it is the only accessible way), it is more informative to directly analyze the conditional probability functions. In Fig. 2, we show $p_{3,\parallel}$ and $p_{3,\perp}$ for $t = 4096$. First we discuss $p_{3,\parallel}$. Several dominant features are present: (i) For all values of r_{01} the average value $\langle x_{12} \rangle$ is negative. Hence, on average a tagged particle moves opposite to the direction it has moved before. This is a direct signature of the cage effect. (ii) The distribution of x_{12} for given r_{01} is to a very good approximation symmetric around $\langle x_{12} \rangle$. Hence, the cage effect can be separated into a deterministic part, driving the particle back with respect to its previous motion, and a stochastic part, allowing for stochastic processes around this new equilibrium position. (iii) For $r_{01} < r_{\text{cage}} \approx 0.8$, one has to a good approximation $\langle x_{12} \rangle = -cr_{01}$ with $c = 0.43$. Hence, for excursions smaller than its own radius, the particle on average is dragged back by a constant fraction of its previous motion. (iv) For $r_{01} > r_{\text{cage}}$, the back-dragging effect slowly decreases. Hence, r_{cage} can be identified with the radius of the cage. Interestingly, the value of r_{cage} is close to the distance for which the dynamics starts to be fully diffusive in Fig. 1(b). (v) The second moment of the distribution of x_{12} as a function of r_{01} , denoted $\sigma_{\parallel}^2(r_{01})$, increases with increasing r_{01} . Particles which move farther than the average particle during some time interval also move farther during the subsequent time interval (apart from the systematic backdragging effect). Hence, it is possible to call such particles *fast*. This is not possible for diffusive dynamics with a single diffusion coefficient where the presence of far-moving particles during some time interval is only a statistical effect.

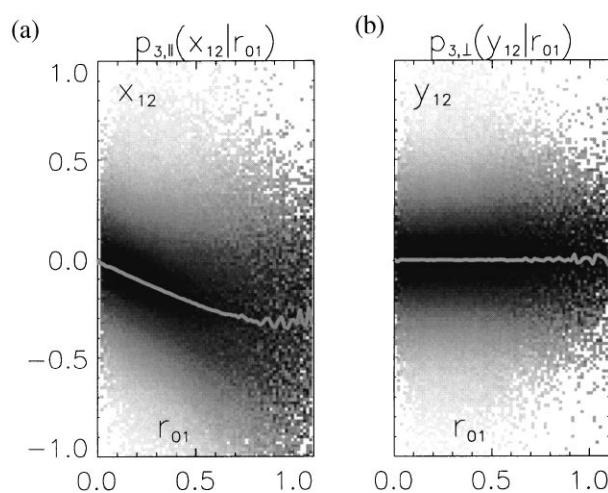


FIG. 2. The conditional probability functions (a) $p_{3,\parallel}(x_{12}|r_{01};t)$ and (b) $p_{3,\perp}(y_{12}|r_{01};t)$ for $t = 4096$, where $x_{12} \equiv \vec{r}_{12} \cdot \vec{r}_{01}$ and $y_{12} \equiv \vec{r}_{12} \cdot \vec{u}_{01}$. The darker areas correspond to high probabilities. The average values $\langle x_{12}(r_{01}) \rangle$ and $\langle y_{12}(r_{01}) \rangle$ are indicated.

From the very definition of $p_{3,\perp}$, one expects $p_{3,\perp}(y_{12}|r_{01};t) = p_{3,\perp}(-y_{12}|r_{01};t)$ for all r_{01} and $p_{3,\parallel}(y_{12}|r_{01};t) \approx p_{3,\perp}(x_{12}|r_{01};t)$ for small r_{01} (in this limit there is no difference between parallel and perpendicular motion). Surprisingly, the width of y_{12} , denoted $\sigma_{\perp}(r_{01})$, hardly depends on r_{01} so that for large r_{01} the value $\sigma_{\parallel}(r_{01})$ is significantly larger than $\sigma_{\perp}(r_{01})$. Hence, the dynamics is strongly anisotropic due to (i) the systematic backdragging effect and (ii) the much larger second moment along the selected direction. This observation may be related to recent results by Donati *et al.*, observing stringlike motional patterns in simulations of Lennard-Jones systems [24,25]. Indeed, these collective features would give rise to quasi-1D dynamics if analyzed in terms of single-particle properties. A precise correlation, however, is beyond the scope of this Letter.

In analogy to Fig. 2, we have calculated the conditional probabilities for all times $t < 10^6$. It turns out that the general shape of the probability distributions is similar to those shown in Fig. 2. The value of r_{cage} turns out to be constant within 10% indicating that the cage is a static concept, independent of time scale. In analogy to the above, we introduce time-dependent $c(t)$, $\sigma_{\parallel}(t, r)$, and $\sigma_{\perp}(t, r)$.

In Fig. 3, we show $\sigma_{\parallel}(t, r)$ and $\sigma_{\perp}(t, r)$ for different values of t and r . In analogy to the discussion of Fig. 2, the significant r dependence of $\sigma_{\parallel}(t, r)$ for all t reveals the presence of fast and slow segments. This effect is more pronounced at longer time scales in agreement with the interpretation of Fig. 1. We checked that the distribution of mobilities is not related to the size of the particle; i.e., small particles on average possess nearly the same mobility as large particles. If we define $r_c(t)$ so that on average 5% of all particles move farther than $r_c(t)$ during t (in Fig. 3 indicated by arrows), then $\sigma_{\parallel}(r_c(t), t)$ and $\sigma_{\perp}(r_c(t), t)$ are a measure of the mobility of the fast particles. The local anisotropies of the fast particles disappear in the microscopic and the α regime.

We define the exponent $\alpha(t)$ as the logarithmic slope of $\sqrt{\langle \Delta r^2(t) \rangle}$ ($\alpha = 0.5$ in the diffusive regime); i.e., $\alpha(t) \equiv$

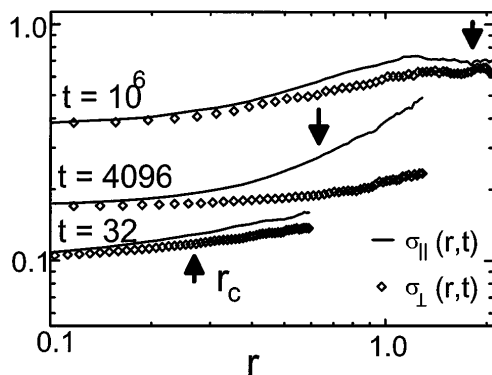


FIG. 3. The dependence of the standard deviations σ_{\parallel} and σ_{\perp} and r_{01} for different times.

$0.5 \ln(\langle r_{02}^2 \rangle / \langle r_{01}^2 \rangle) / \ln 2$. In Fig. 4, we plot $0.5 - c(t)$ and $\alpha(t)$. On a qualitative level, both quantities display a similar time dependence. In the region of anomalous diffusion ($\alpha \approx 0.1$), the cage is very efficient in pushing back particles to their original position ($c \approx 0.4$). Indeed, it is possible to connect c and α even on a quantitative level. We assume that (i) $p_{3,\parallel}(x_{12}|r_{01}, t) \propto \exp\{-k_2(t)[x_{12} + c(t)r_{01}]^2\}$ and (ii) $p_{3,\perp}(y_{12}|r_{01}, t) \propto \exp[-k_2(t)y_{12}^2]$. This choice approximately describes the numerical results for $r < r_{\text{cage}}$ as expressed in Fig. 2 if the dependence of $\sigma_{\parallel,\perp}(t, r)$ on r is neglected. This choice implies that the probability p_2 to move by \vec{r}_{01} during time t is Gaussian; i.e., $p_2(\vec{r}_{01}, t) \propto \exp[-k_1(t)r_{01}^2]$ with $k_2(t) = k_1(t)[1 - c(t)^2]$. After some straightforward calculation, one obtains $\langle r_{01}^2 \rangle = 2/k_1(t)$ and $\langle r_{02}^2 \rangle = 4[1 - c(t)]/k_1(t)$. From these values the logarithmic slope of the mean-square displacement turns out to be

$$\alpha_{\text{est}}(t) = 0.5 + \ln[1 - c(t)] / \ln(4.0). \quad (1)$$

As shown in Fig. 4, we calculate $\alpha_{\text{est}}(t)$ from the simulated values of $c(t)$. For $t < 10^4$, the agreement is very good. This shows that the cage effect fully accounts for the observed anomalous diffusion. For $t > 10^4$, more particles leave the cage ($r > r_{\text{cage}}$) leading to a stronger increase of $\sqrt{\langle \Delta r^2 \rangle}$ than expected from the slope $c(t)$, i.e., $\alpha(t) > \alpha_{\text{est}}(t)$. Interestingly, the simple model of Brownian dynamics in an isotropic harmonic potential strictly fulfills assumptions (i) and (ii) [26]. Hence, one has a simple model characterizing the cage. This observation may come as a surprise since for hard spheres the concept of harmonic potential wells around some local energy minima does not exist (compare, however, Ref. [27]). We checked that describing the case by a boxlike effective potential does not account for the features seen in Fig. 2.

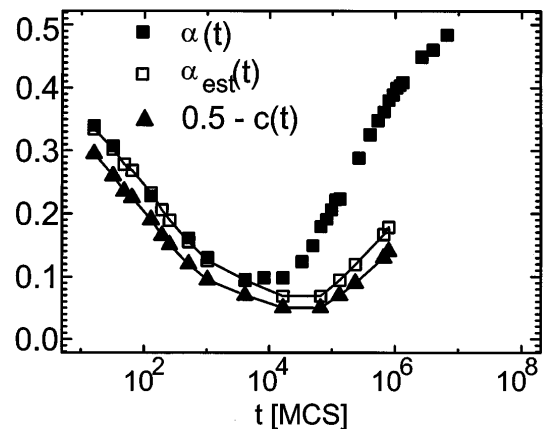


FIG. 4. The dependence of the initial slope $c(t)$ [extracted from $p_{3,\parallel}(x_{12}|r_{01};t)$ for $r_{01} < r_{\text{cage}}$], the exponent $\alpha(t)$ characterizing the local slope of the mean-square displacement with time [extracted from Fig. 1(b)], and the estimation α_{est} from $c(t)$ on the basis of Eq. (1).

Now we are in a position to formulate a rather detailed scenario of the dynamics of hard spheres close to the glass transition. At short times ($t < 100$), the dynamics is mainly diffusive. At longer times ($t \approx 10^3$), the dynamics can be separated into a deterministic part, due to the strong back-and-forth correlations resulting from the restrictions of the cage, and a stochastic part, reflecting the local mobility. On a local scale, the mobility is highly anisotropic, indicating the presence of some “weak” local directions, i.e., an anisotropic harmonic potential. At still longer times, two additional effects occur. First, a significant fraction of particles is successful in leaving the cage as seen from the difference between $\alpha(t)$ and $\alpha_{\text{est}}(t)$ for $t > 10^4 \equiv t_1$. Second, the final decrease of $c(t)$ for $t > 10^5 \equiv t_2$ indicates that the cage effect becomes weaker. Qualitatively, this can be explained by the fact that on longer time scales the cage may relax and, hence, adjust to the new position of the particle. It is plausible that $t_2 \gg t_1$ since the particles forming the cage must have been able to escape their own cage as well. Both effects, starting at t_1 and t_2 , respectively, are not included in the simple representation of the cage as a harmonic potential. Finally, in the α regime ($t > 10^6$), most particles have left their cage, and the dynamics is mainly diffusive ($\alpha \approx 0.5$). However, the dynamics is still nontrivial. First, one observes a systematic backdragging effect ($c > 0$) rendering the concept of a cage useful even in the α regime, and, second, the strong dependence of $\sigma_{\parallel, \perp}$ on r indicates a broad distribution of mobilities. Only for much longer times, the particles may experience different environments so that the heterogeneities are averaged out. Then the dynamics of a tagged particle can be described by purely diffusive dynamics with a single diffusion constant.

It remains an interesting goal to extend this analysis beyond the single-particle picture and to get information, e.g., about the spatial patterns. This would allow comparison with collective properties, as, e.g., obtained for the cage effect in Ref. [3]. However, already the present analysis has shown that consideration of multitime correlations contains relevant information which allows a simple and model-free analysis of complex dynamical processes like those occurring close to the glass transition.

We gratefully acknowledge helpful discussions with S. Buechner, M. Fuchs, R. Schilling, W. Kob, and H. W. Spiess. This work has been supported by the DFG (SFB 262).

*Corresponding author.

- [1] M.D. Ediger, C.A. Angell, and S.R. Nagel, *J. Phys. Chem.* **100**, 13 200 (1996).
- [2] *Structure and Dynamics of Glasses and Glass Formers*, edited by C.A. Angell, K.L. Ngai, J. Kieffer, T. Egami, and G.U. Nienhaus, MRS Symposia Proceedings No. 455 (Materials Research Society, Pittsburgh, 1997).
- [3] J.L. Barrat, W. Götze, and A. Latz, *J. Phys. Condens. Matter* **1**, 7163 (1989).
- [4] W. Götze and L. Sjögren, *Rep. Prog. Phys.* **55**, 241 (1992).
- [5] M. Fuchs, I. Hofacker, and A. Latz, *Phys. Rev. A* **45**, 898 (1992).
- [6] T. Scheidsteiger and R. Schilling, *Phys. Rev. E* **56**, 2932 (1997).
- [7] K. Schmidt-Rohr and H.W. Spiess, *Phys. Rev. Lett.* **66**, 3020 (1991).
- [8] A. Heuer, M. Wilhelm, H. Zimmermann, and H.W. Spiess, *Phys. Rev. Lett.* **75**, 2851 (1995).
- [9] R. Boehmer, G. Hinze, G. Diezemann, B. Geil, and H. Sillescu, *Europhys. Lett.* **36**, 55 (1996).
- [10] A. Heuer and K. Okun, *J. Chem. Phys.* **106**, 6176 (1997).
- [11] C.T. Moynihan and J. Schroeder, *J. Non-Cryst. Solids* **160**, 52 (1993).
- [12] M.T. Cicerone and M.D. Ediger, *J. Chem. Phys.* **103**, 5684 (1995).
- [13] B. Schiener, R. Böhmer, A. Loidl, and R.V. Chamberlin, *Science* **274**, 752 (1996).
- [14] S.C. Kuebler, A. Heuer, and H.W. Spiess, *Phys. Rev. E* **56**, 741 (1997).
- [15] R. Richert, *J. Phys. Chem. B* **101**, 6323 (1997).
- [16] L.V. Woodcock and C.A. Angell, *Phys. Rev. Lett.* **47**, 1129 (1981).
- [17] H. Löwen, *Phys. Rep.* **237**, 249 (1994).
- [18] B. Cichocki and K. Hinsen, *Physica (Amsterdam)* **166A**, 473 (1990).
- [19] W. Schaertl and H. Sillescu, *J. Stat. Phys.* **74**, 687 (1994).
- [20] W. van Meegen and P.N. Pusey, *Phys. Rev. A* **43**, 5429 (1991).
- [21] I. Moriguchi, K. Kawasaki, and T. Kawakatsu, *J. Phys. II (France)* **3**, 1179 (1993).
- [22] J.L. Barrat and J.P. Hansen, *J. Phys. (Paris)* **47**, 1547 (1986).
- [23] The present definitions are identical to those in [10] for isotropic systems, as considered here.
- [24] C. Donati, J.F. Douglas, W. Kob, S.J. Plimpton, P.H. Poole, and S.C. Glotzer, *Phys. Rev. Lett.* **80**, 2338 (1998).
- [25] W. Kob, C. Donati, S.J. Plimpton, P.H. Poole, and S.C. Glotzer, *Phys. Rev. Lett.* **79**, 2827 (1997).
- [26] M. Doi and S.F. Edwards, *The Theory of Polymer Dynamics* (Clarendon, Oxford, 1986).
- [27] F. Sciortino, P. Gallo, P. Tartaglia, and S.H. Chan, *Phys. Rev. E* **54**, 6331 (1996).